Mapping groundwater reserves in northwestern Cambodia with the combined use of data from lithologs and time-domain-electromagnetic and magnetic-resonance soundings

Article *in* Hydrogeology Journal · January 2018

DOI: 10.1007/s10040-018-1726-1

CITATIONS
0

READS
91

4 authors, including:

Rémi Valois
Centro de Estudios Avanzados en Zonas Áridas, La Serena, Chile
14 PUBLICATIONS **248** CITATIONS
SEE PROFILE

Jean-Michel Vouillamoz
Institute of Research for Development
68 PUBLICATIONS **898** CITATIONS
SEE PROFILE

Mapping groundwater reserves in northwestern Cambodia with the combined use of data from lithologs and time-domain-electromagnetic and magnetic-resonance soundings

Remi Valois, Jean-Michel Vouillamoz, Sambo Lun & Ludovic Arnout

Hydrogeology Journal
Official Journal of the International Association of Hydrogeologists

ISSN 1431-2174

Hydrogeol J
DOI 10.1007/s10040-018-1726-1

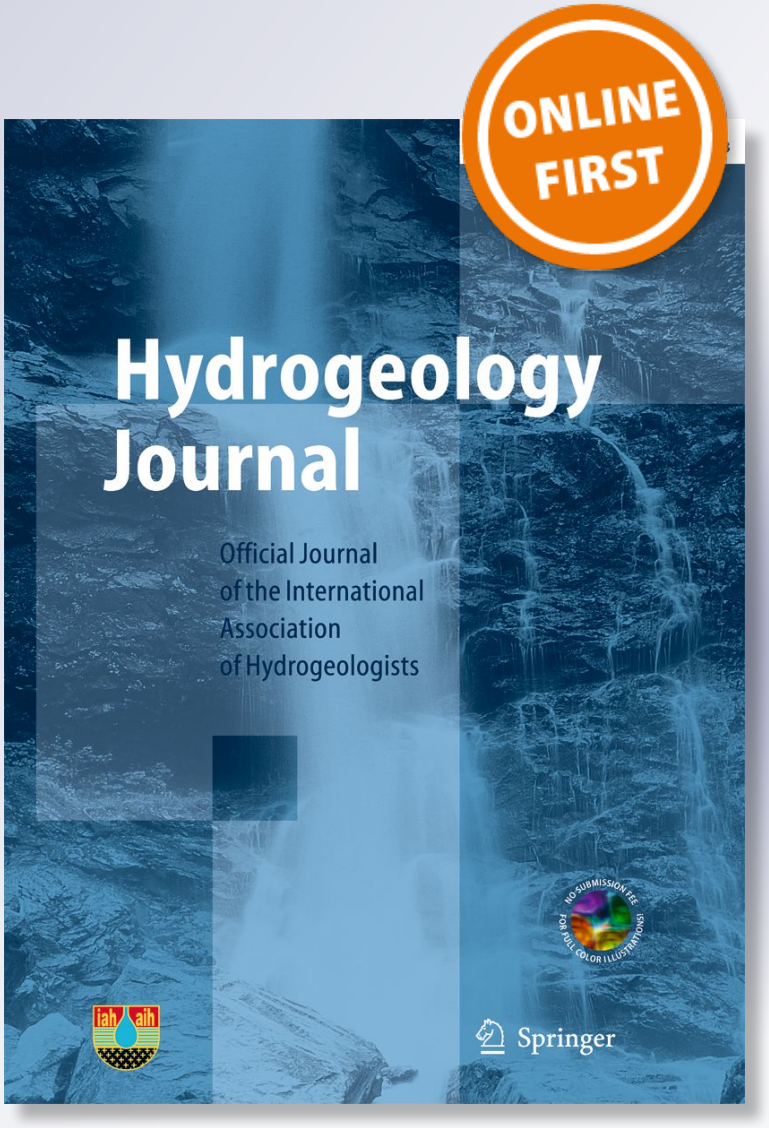

Springer

Hydrogeology Journal
https://doi.org/10.1007/s10040-018-1726-1

REPORT

Mapping groundwater reserves in northwestern Cambodia with the combined use of data from lithologs and time-domain-electromagnetic and magnetic-resonance soundings

Remi Valois[1,2] · Jean-Michel Vouillamoz[3] · Sambo Lun[2,4,5] · Ludovic Arnout[2]

Received: 29 June 2017 / Accepted: 7 January 2018

Abstract
Lack of access to water is the primary constraint to development in rural areas of northwestern Cambodia. Communities lack water for both domestic and irrigation purposes. To provide access to drinking water, governmental and aid agencies have focused on drilling shallow boreholes but they have not had a clear understanding of groundwater potential. The goal of this study has been to improve hydrogeological knowledge of two districts in Oddar Meanchey Province by analyzing borehole lithologs and geophysical data sets. The comparison of 55 time-domain electromagnetic (TEM) soundings and lithologs, as well as 66 magnetic-resonance soundings (MRS) with TEM soundings, allows a better understanding of the links between geology, electrical resistivity and hydrogeological parameters such as the specific yield (S_y) derived from MRS. The main findings are that water inflow and S_y are more related to electrical resistivity and elevation than to the litholog description. Indeed, conductive media are associated with a null value of S_y, whereas resistive rocks at low elevation are always linked to strictly positive S_y. A new methodology was developed to create maps of groundwater reserves based on 612 TEM soundings and the observed relationship between resistivity and S_y. TEM soundings were inverted using a quasi-3D modeling approach called 'spatially constrained inversion'. Such maps will, no doubt, be very useful for borehole siting and in the economic development of the province because they clearly distinguish areas of high groundwater-reserves potential from areas that lack reserves.

Keywords Cambodia · Geophysical methods · Resistivity · Magnetic resonance sounding · Groundwater exploration

Introduction

Oddar Meanchey province is a remote area located in northwestern Cambodia, far from the traditional developed rice plains of the Mekong River or Tonle Sap Lake. Inhabitants depend primarily on one rain-fed rice crop per year, and potable water is not accessible in many parts of the province (Bunthan 2006; Gupta 2001). Streams usually run dry during the dry season and the precipitation from the monsoon that is stored in ponds and dams is highly vulnerable to surface pollution. Shallow aquifers do not provide much water and boreholes drilled by NGOs and governmental agencies can supply only domestic uses (Vouillamoz et al. 2015). Such aquifers are mainly located in claystones and fine sandstones with low specific yield, which could be caused by a high clay content and a low fracture density; furthermore, the population has more than tripled since the end of the civil war in 1999; it reached 71,000 inhabitants in 2008 (National Institute of Statistics 2009). Consequently, the pressure on water resources increased. Newcomers to Oddar Meanchey province have found almost no drinking-water infrastructure: in 1998, only 2.5% of the population had access to a protected water source, whereas the national rate was about 30% (National Institute of Statistics 2009).

✉ Remi Valois
remi.valois1@gmail.com

1 Centro de Estudios Avanzados en Zonas Áridas (CEAZA), 35 av Raúl Bitran, La Serena, Chile

2 French Red Cross, 4 rue Didot, Paris, France

3 IRD, UMR IGE (Univ. Grenoble Alpes/CNRS/IRD/Grenoble-INP), 38000 Grenoble, France

4 Department of Environment Systems, Graduate School of Frontier Sciences, the University of Tokyo, 5-1-5 Kashiwanoha, Kashiwa, Chiba 277-8563, Japan

5 Department of Rural Engineering, Institute of Technology of Cambodia, Phnom Penh, Cambodia

Published online: 23 January 2018

Governmental and aid agencies are supporting borehole drilling projects to supply communities with water all year round; nevertheless, the groundwater potential has hardly been investigated (e.g., Rasmussen and Bradford 1977) and no spatial assessment of groundwater resources has been conducted in Oddar Meanchey province because of civil war. Vouillamoz et al. (2015) is the first study dealing with the potential of groundwater to meet irrigation needs, and Valois et al. (2017) focuses on the assessment of groundwater recharge. In addition, mapping groundwater reserves is a novel goal in northwestern Cambodia because most Cambodian groundwater publications focus on alluvial units of the Mekong River that are vulnerable to arsenic pollution (Berg et al. 2007; Benner et al. 2008). Landon (2011) confirms that groundwater studies must be also carried out in other regions of Cambodia because much uncertainty surrounds groundwater recharge and reserve assessment in the entire country. MRD and JICA (2002) conclude on the extremely urgent formulation of the water supply plan through groundwater development because of the drying up of surface reservoirs. The limited use of groundwater in many places in Cambodia is attributed to reasons such as limited knowledge of the resource and its sustainability, as mentioned by Johnston et al. (2013) and Kummu et al. (2014). Raksmey et al. (2010) deals with the influence of flooding on groundwater flow in central Cambodia, whereas the studies of Vouillamoz et al. (2002, 2012, 2013, 2015) focus on the assessment of aquifer hydraulic properties through the use of magnetic resonance sounding (MRS).

The goal of this study is to use geophysical methods to map groundwater reserves in two districts of Oddar Meanchey province. Geophysical methods have successfully contributed to groundwater characterization, in particular electromagnetic methods (Bedrosian et al. 2016; Chongo et al. 2015a, b; Lenat et al. 2000; Lienert 1991; MacNeil et al. 2007; Pryet et al. 2012) and MRS (Baroncini-Turricchia et al. 2014; Legchenko 2013; Lubczynski and Roy 2007; Vouillamoz et al. 2002, 2013). The extensive time-domain electromagnetics (TEM) survey carried out in this study makes it possible to explore resistivity in 3D in the area, whereas MRS is able to assess empirical relationships between geophysical and hydrogeological parameters. This better understanding of hydrogeophysical issues has allowed for development of an innovative workflow, which aims to create the first groundwater reserves maps for the Oddar Meanchey province.

Area of investigation

The study area (about 3,380 km^2) covers the districts of Along Veng and Trapeang Prasat, located in the eastern part of Oddar Meanchey province (Fig. 1). Population of the two districts was 71,000 in 2008, which was 30% of the total population of the province (National Institute of Statistics 2009). The area is a flat plain except for some smooth isolated hills called *phnom* and the 300-m cliffs that mark the Cambodia-Thailand border. The cliffs are the Dangrek Mountains, located at the edge of a sandstone escarpment, and composed of sandstones dating from Upper Triassic to Lower Cretaceous (Dottin 1972). The beds dip to the north (5–8°) and they are composed of conglomerates, fine- to coarse-grained sandstone, variegated siltstone, and argillites. No evidence of tectonic faulting has been observed in the sandstones (Dottin 1972). In the study area, the Upper Triassic to Lower Cretaceous series was eroded (they crop out clearly further south) and then covered by Pleistocene to Holocene age alluvium, which consists of clay, silt, and sand. An E–NE to W–SW oriented anticline has probably affected geological units in the southern part of the study area. This anomaly should place Triassic sandstones in contact with Permian limestones and Pleistocene sands (Fig. 1; Bouche et al. 1990). The Paleozoic substratum locally crops out as schist phnoms in the western part of the study area (Dottin 1972). Several boreholes encountered volcanic rocks (probably trachytes) attributed to the same geological period as the upper sandstones which crop out further southeast of the province (Dottin 1972).

The area is drained towards the Tonle Sap Lake, which is the 18th largest lake of the world and the largest source of freshwater in southeast Asia. Most rivers dry up after the rainy season and perennial runoff is non-existent. Lowlands are normally used to grow rice during the rainy season, whereas uplands are more forested, bushy, or cultivated with cassava.

Materials and methods

The study was implemented over a 6-year period (2009–2014) using several methods including statistical analysis of a database of 55 wells with lithologs and TEM soundings, 66 combined MRS and TEM soundings, and a total of 612 TEM soundings.

Borehole lithologs

The Cambodian Red Cross and French Red Cross offices had in their possession 55 drilling reports that included lithologs used to complement the description of local geology prepared by Dottin (1972). The lithologs were drawn by the drillers on the basis of cuttings. In addition to lithologic descriptions, the depths of water inflow were also recorded during drilling works from 2009 to 2011. They correspond to depths where the outflow from the drilling holes increases visually. Boreholes with no water inflow or with an instantaneous yield lower than 0.5 m^3 h^{-1} were considered as negative. For this reason, 25 were abandoned. Groundwater

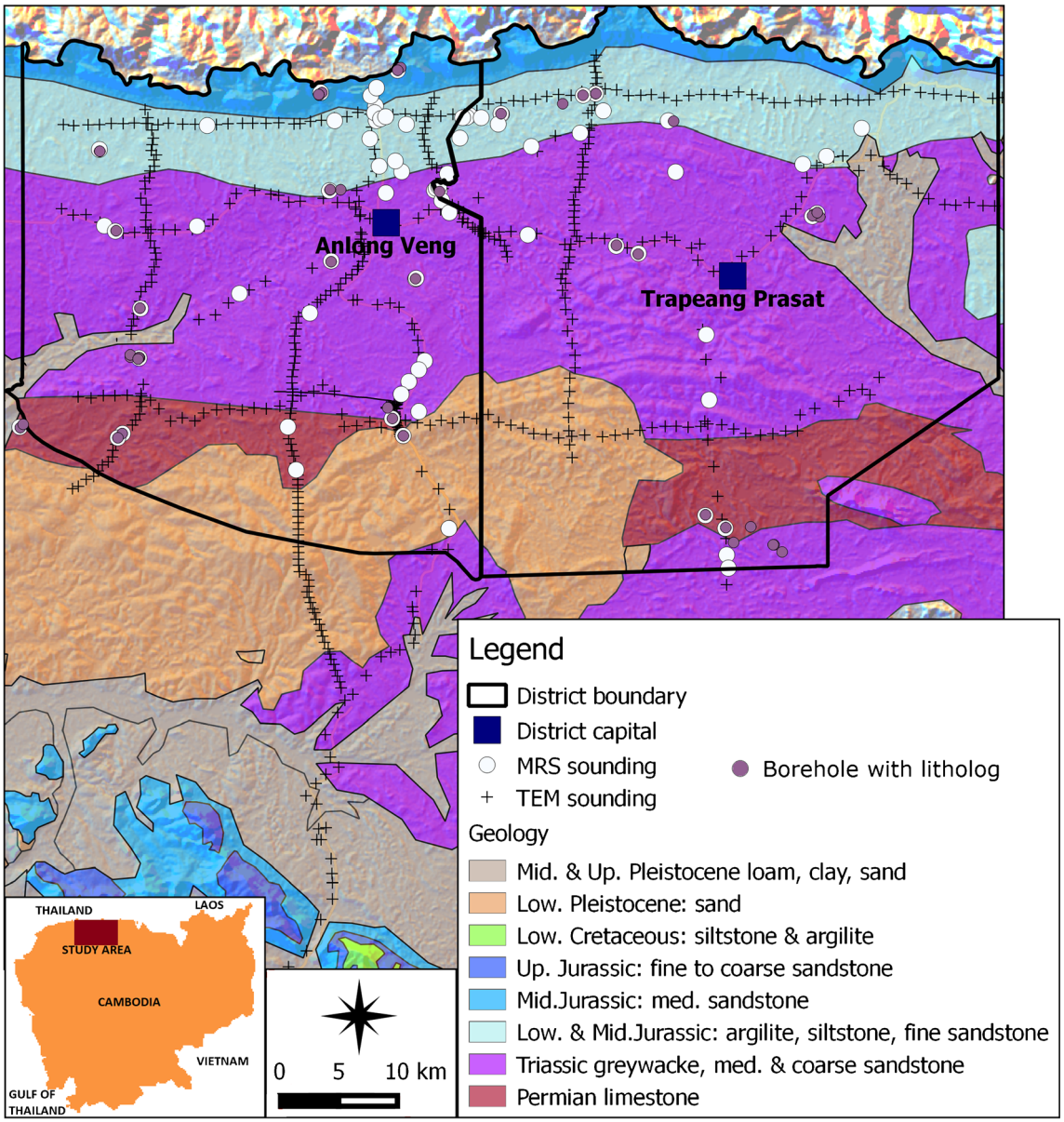

Fig. 1 Geological map in northwest Cambodia, modified from Bouche et al. (1990). The northern district boundaries mark the border between Thailand and Cambodia

electrical conductivity was measured with a HANNA 9828 multi-parameter probe.

TEM

The time-domain (or transient) electromagnetic (TEM) sounding is used to characterize the vertical distribution of electrical resistivity of geological materials. This method was applied here to gain information on hydrogeological units (Nabighian 1988, 1991; Kirsch 2006; Chongo et al. 2015a, b). Ground exploration using TEM commonly involves placing a square loop on the targeted area and performing soundings or profiling (McNeill 1980). The transmitter passes a DC current through the loop, which produces a primary magnetic field. The current is quickly turned off, thereby interrupting the primary magnetic field. Based on the principles of electromagnetism, secondary currents can be induced in the subsurface by a time-varying electromagnetic field. Secondary magnetic fields generated by secondary currents can then also be measured using a loop (Nabighian 1988). In this study, the TEM FAST 48HPC was used in a coincident-loop configuration; the same loop acted both as transmitter (Tx) and receiver (Rx; Barsukov et al. 2006). The high productivity of the TEM FAST equipment in a light, portable unit that uses a single Rx-Tx loop is an important advantage. The coincident-loop configuration accelerates fieldwork (Legchenko et al. 2009), which was usually undertaken using a backpack and a motorbike. In this study, a total of 612

soundings were carried out (Fig. 1) with loop side sizes of 25 m (7% of the 612 soundings), 50 m (60%), and 100 m (33%). The loop side size was in reality adapted to local conditions such as trees, topography, and houses. Measurements were stacked at least 10 times to increase the signal-to-noise ratio; in addition, values with relative errors above 5% were disregarded.

TEM data were inverted using the AarhusInv inversion software (Auken et al. 2015). This software makes it possible to model and invert large sets of TEM soundings. Spatially constrained inversion (SCI) was used, which produces quasi-3D resistivity modeling of TEM data using a 1D vertical forward solution (Viezzoli et al. 2008). Spatial constraints were set between the model parameters of the nearest neighboring soundings. Data sets, models, and spatial constraints are inverted as one system. The constraints are built using Delaunay triangulation as explained in Viezzoli et al. (2008) which ensures automatic adaptation to data density variations. SCI applies horizontal constraints to ensure lateral continuity, which improves resolution of model parameters for single stations that are not well resolved by the data from that station alone. In profile-oriented data sets, SCI ensures a connection between adjacent lines by means of across-line constraints, which ensures continuity of geological units (Viezzoli et al. 2008). Such a method is relevant in the context of this study because of the spatially heterogeneous dataset and because a certain geological continuity is expected on the geological maps (Fig. 1).

Setting the strength of these constraints is an important step because constraints will impact the inversion results and need to reflect the expected variations in the geologic model. The constraints applied are largely based on studies of 3D forward modeling of complicated geologic models followed by laterally constrained inversion (Auken et al. 2005). The strength of the constraints is distance dependent, as shown in Eq. (1):

$$C(d) = 1 + (C_{\mathrm{ref}} - 1)\left(\frac{d}{d_{\mathrm{ref}}}\right)^{a} \quad (1)$$

where d represents the distance between two constrained soundings, d_{ref} the reference distance, and C_{ref} the reference constraint value. The reference distance is the typical separation between adjacent soundings, which ranges from 250 to 1 km, depending on the profiles. The reference constraint is the value to which the strength of the constraints is set in case of soundings that are closer than the reference distance (Viezzoli et al. 2008). The exponent a determines how the constraints loosen up with distance. Numerous simulations not presented in this study were carried out to assess the best a, d_{ref} and C_{ref} that allow an acceptable fit between observed and modeled data, as well as geological continuity. For this purpose, smooth 1D models of 20 fixed-thickness layers with initial resistivities of 20 Ω m, and a, d_{ref} and C_{ref} set to 1.5, 500 m and 0.5, respectively, were used. Smooth models were chosen because drilling data show smooth variations between geological units such as claystones, siltstones, and sandstones.

The methodology developed by Pryet et al. (2012) was used to build a 3D resistivity model. Kriging was used to interpolate the 21 model parameters on a horizontal 2D grid (i.e., the 20 resistivity layers and the depth of investigation calculated from the final models). The 3D grid was then created from the interpolated data to allow 3D visualization and advanced interpretation with Paraview software, for example.

MRS

MRS is used to characterize the water content vertical distribution of underground materials and to gain information on the pore size as well (Schirov et al. 1991, Trushkin et al. 1995, Shushakov 1996). MRS is based on exciting the nuclei of hydrogen atoms in groundwater molecules at the Larmor frequency, which depends on the geomagnetic field. MRS equipment allow measurements of the magnetic resonance signal generated by the precessing nuclei after the stimulation signal is terminated (Vouillamoz et al. 2008). The physical foundation of the method is discussed in numerous publications (e.g., Legchenko and Valla 200a). Geophysical parameters estimated from signals recorded in the field are the MRS-determined water content (θ_{MRS}) and decay time constants (T_2^*) associated with water in each inversion layer. The latter is linked to the average pore size that contains groundwater (Schirov et al. 1991).

Like the TEM soundings, MRSs were carried out with a coincident square loop acting as both transmitter and receiver. An AC current passes through the loop, which creates an electromagnetic field at the Larmor frequency. Loop side sizes range from 50 m with two loop turns, to 100 m with one loop turn, depending mainly on obstacles at the survey sites. This study used 10–16 different pulse moments, which range from 10 to 7,000 A ms. The measurements were performed with a Numis$^{\mathrm{plus}}$ (Iris instruments) device, thus giving an investigation depth of 50–80 m below ground level with these loop configurations and in the electrically conductive media of the studied area (Legchenko et al. 2002; Hunter and Kepic 2005, Bernard 2007). While carrying out the measurements, special care had to be taken to obtain high quality MRS measurements because water content is generally low at the site, as seen in the study of Vouillamoz et al. (2015) and, as a result, the MRS signal could be low as well. For this reason, it could take from a half-day up to 3 days to complete a high quality MRS because signal stacking (150–500 stacks) was the only remedy available for obtaining a good signal-to-noise ratio. The early morning hours seemed to be the best period for doing MRS because at this time, the electromagnetic noise appeared to be low (less than 12 nV in the loop). In the study area, 66 good quality MRS were carried out. Data with signal-

to-noise ratio less than 2 were disregarded, which yields an average signal-to-noise ratio of approximately 2.8. A positive side effect of measuring only in the early mornings is the relative stability of the geomagnetic field, which should not vary on its full daily range; moreover, a tool was used during the inversion process to limit the effects of geomagnetic field variation on the resonance frequency of hydrogen atoms, as described in Legchenko et al. (2016). This tool takes into account the frequency offset between the frequency of the measured signals and the frequency in the transmitting signal for each pulse. During one pulse, the geomagnetic field should vary rather smoothly, and should not require such a correction.

Inversion of MRS data was done using Samovar V11.43 software (Legchenko et al. 2008), which provides 1D vertical models of θ_{MRS} and T_2^* by adjusting the modeled and measured signal amplitudes and decay times for each pulse. The chosen MRS result is the single water-layer model which fits well with the field records. The uncertainty in the MRS results is calculated by estimating the space of acceptable solutions (i.e., the equivalence analysis). The solutions are considered acceptable if the difference ε between the field data and the calculated solution is lower than a threshold value, which is given by the noise in the data.

Vouillamoz et al. (2012) conducted MRS at nine experimental sites in the studied area to compare MRS decay time T_2^* [ms] with specific yield S_y [−] obtained from pumping tests, and they found:

$$\begin{cases} if\ T_2^* < 130\ ms \Rightarrow S_y \rightarrow 0 \\ if\ \ T_2^* > 130\ ms \Rightarrow S_y = 1.8.10^{-4}\ T_2^* - 0.02 \end{cases} \quad (2)$$

Groundwater reserves can therefore be computed from MRS results by multiplying the saturated aquifer thickness by S_y.

Results

Borehole statistics

Fifty-five boreholes were drilled and numerous geological layers were identified in the lithologs. Taking into consideration the lithology of the layers, the resistivity obtained from TEM soundings, and the rate at which water inflow is observed to be present, four kinds of medium were identified (Fig. 2):

- Conductive surface layers (clay, sand, and laterite) with water-inflow-presence rates lower than 22%. Their bottoms have an average depth of about 8 m and a maximum depth of 28 m.
- Sandstone D, which appears to be an unfavorable medium to target for the purposes of groundwater extraction. It differs from classic sandstone because it is located in the Dangrek mountains at higher elevation and its resistivity is very high.
- Claystone, mudstone, and schist that span a large resistivity range with an average water-inflow-presence rate.
- Sandstone, crystalline rock and trachyte layers, which reveal water-inflow-presence rates above 50%. These rocks are associated with average to high resistivities.

Layer resistivities were then correlated with the layer-top's elevation, and the media were separated into three groups: those with water inflow, those with no water inflow located above the water-inflow layers, and those corresponding to negative boreholes (Fig. 3). Figure 3 shows that resistive media below the elevation of 56 m and with resistivity greater than 36 Ω m are associated only with water-inflow layers. These layers are mainly composed of schist, with some crystalline rock, mudstone, and trachyte. A similar pattern was observed in claystone layers: those with resistivity greater than 14 Ω m and located below 80 m elevation are indeed all associated with water inflow. Moreover, it should be noted that water inflow was never detected for layers of less than 13 Ω m resistivity.

Combined MRS and TEM soundings

A total of 80 MRSs were carried out over the studied area, as shown in Fig. 1. The results of a representative MRS are shown in Fig. 4, where raw and calculated data are on shown in Fig. 4a and the corresponding models are in Fig. 4b. Thus, one can see that a shallow aquifer of about 20 m depth with a MRS water content of 1.1% produces a signal of about 40 nV in the conditions of this study. In order to estimate the reliability of the inverted parameters, an exploration was carried out of the one-water-layer parameters in terms of space (aquifer position and thickness, and the corresponding MRS water content). Only the maximal and minimal water-content models (black and black-dashed lines, respectively, in Fig. 4b) whose RMSEs are less than 110% of the best RMSE fit model (red lines) were kept. The error on the water content is about 15% of the estimated value, which is in accordance with the value of 22% found by Vouillamoz et al. (2012) in the same studied zone.

With the 80 MRSs, the median MRS water content is approximately 1.1% and the maximum value recorded in the area is 14% (Fig. 5). Nevertheless, previous studies (Vouillamoz et al. 2015, Valois et al. 2017) suggest using the T_2^* – S_y approach as mentioned earlier, because clayey materials may have a high MRS water content and a very low S_y. Using this approach for drilling boreholes is advantageous because it has a higher success rate than results obtained when using only the MRS water content (French Red Cross 2015;

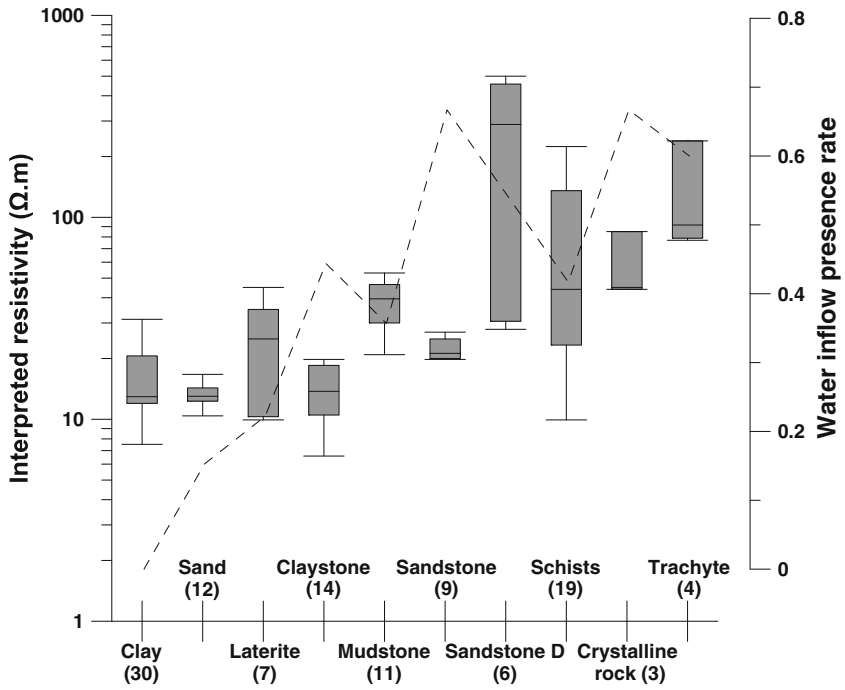

Fig. 2 Maximum, upper quartile, median lower quartile and minimum resistivities for the geologic units encountered during drilling. The dashed line represents the water-inflow-presence rate (ratio of layers with water inflow to layer number). The numbers below the geologic description are the layer numbers

Vouillamoz et al. 2015). The pore size linked to T_2^* seems to be the limiting factor for high S_y, as stated in these studies. T_2^* ranged over a large amplitude of values: from 90 to 330 ms; thus, S_y ranges from 0 to 3% with a median value of about 0.5%. The average aquifer thickness is about 16 m with a maximum value of 80 m, which corresponds to the maximum depth of investigation.

Among the 66 locations where joint MRS and TEM soundings were carried out, 17 lithologs were available. Specific yields and resistivities for each layer could thus be identified (Fig. 6). For the remaining joint soundings, resistivities of the different TEM models were averaged over the aquifer thickness obtained from MRS. By comparing S_y, the resistivity and the elevation of each sounding or layer, four resistivity-elevation classes with different behaviors were established, as summarized in Table 1:

- A very conductive class (class 1) with no specific yield.
- A second conductive class with a 53% probability of obtaining a non-zero S_y of 0.77% on average.
- A third class with resistive medium above a 56-m elevation, which has a 64% probability of non-zero S_y and an average S_y of 0.85%. This class does, in fact, have better S_y properties because MRS appears to not always be

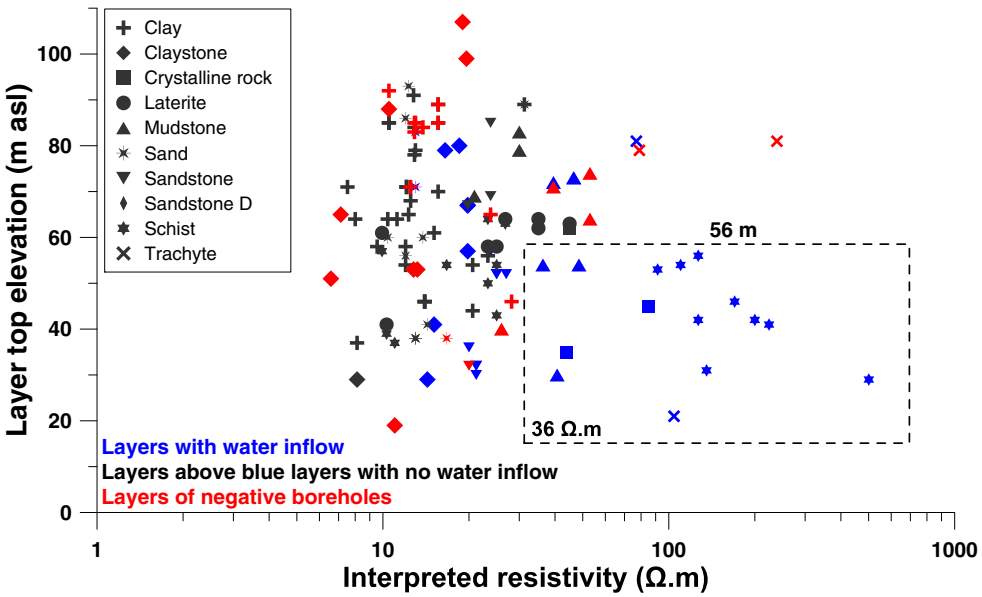

Fig. 3 Relationship between layer resistivity, layer elevations, and the water-inflow presence. Water-inflow presence is clearly noticed in the dashed-line rectangle

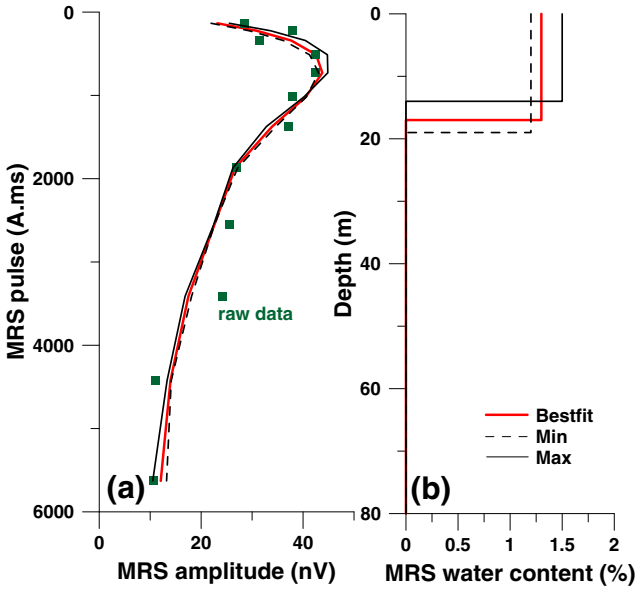

Fig. 4 Representative MRS results at O'Kokikrum village: **a** Raw and calculated data, **b** models used to calculate data with a T2* of 180 ms. RMSE values are 3.84, 4.05 and 3.93 nV for the Bestfit, Min and Max models respectively

sensitive to water inflow (e.g., the two blue squares with no S_y but with water inflow in Fig. 6).

– A fourth class with resistive medium at low elevation, always associated with water inflow, strictly positive S_y, and the best S_y value of approximately 1.06% on average.

The first and last classes are illustrated in Fig. 7, which shows that class 1 conductive layers (less than 10 Ω m in Fig. 7a) are not associated with sufficient free water to create MRS signals (Fig. 7b). This results in the absence of S_y, however, on the other hand, the shallow resistive layer of class 4 (41 Ω m) is associated with strong MRS amplitudes and a high S_y value.

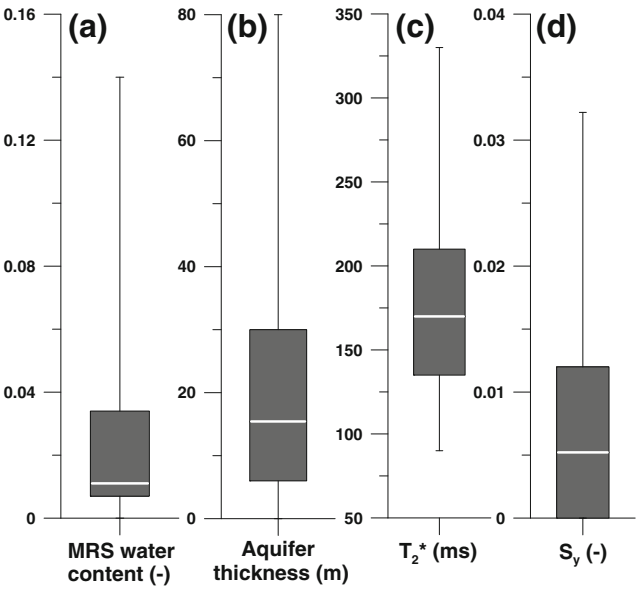

Fig. 5 Maximum, upper quartile, median, lower quartile and minimum on the 80 MRS results. Included are zero values when MRS signal was too weak (**a**, **b**, **d**). T_2^* graph (**c**) takes into account only soundings with sufficient MRS signal for T_2^* assessment

Up-scaling from the TEM survey

The SCI method described in section 'Materials and Methods' was used to invert the 612 TEM soundings; the locations are displayed in Fig. 1. Sounding locations reflect the roads in the two districts because roads allow access to the fields studied. The inversion fits the data well in 99% (i.e., 604 soundings with a RMSE lower than the measurement standard deviation) of the total number of soundings. For each resistivity value, thicknesses of layers corresponding to this resistivity value were summed. Results are displayed in Fig. 8 using all resistivity layers extracted from the SCI. The resistivity distribution shows a peak of about 12 Ω m with several lower resistivity occurrences and many higher resistivity ones. The log-average resistivity is about 21 Ω m.

The shallow resistivity map (Fig. 9) highlights media of more than 80 Ω m resistivity in high-elevation areas at the middle of the map, which may represent non-saturated Pleistocene sands (Fig. 1). Conductive zones of about 10 Ω m are found at low elevations at the middle and in the southern part of the map. The southern bodies may reflect middle and upper Pleistocene clays.

At depth, resistivity patterns are quite different and show larger areas of conductive media from the north-western edge of the studied area and along a E–SE axis (Fig. 10). Moreover, locations with surface resistive bodies on the eastern part of the map (Fig. 9) show resistivities lower than 10 Ω m at depth (Fig. 10). These conductive bodies may be linked to rich clayey material such as Triassic claystone, for example. Locations of resistive bodies greater than 80 Ω m in the western part of the study area are in good agreement with the Permian limestone shown on the geological map (Fig. 1). Resistive zones in the southeast should be Permian limestones as well, although the Permian limestone as delimited by the geological map (Fig. 1) is located in a slightly different area. Some crystalline rocks have been found in borehole cuttings and schist phnoms outcrops have been observed in this area. Resistivities of limestones, crystalline rocks, and schists may correspond to those high resistivities (Fig. 2; Guéguen and Palciauskas 1997).

S_y-reserves mapping

Groundwater reserves were computed using the 3D resistivity model and the relationship between resistivity and S_y. Each vertical resistivity distribution was transformed into a vertical S_y distribution depending on the four classes described previously (Table 1). S_y was then summed on each vertical from the

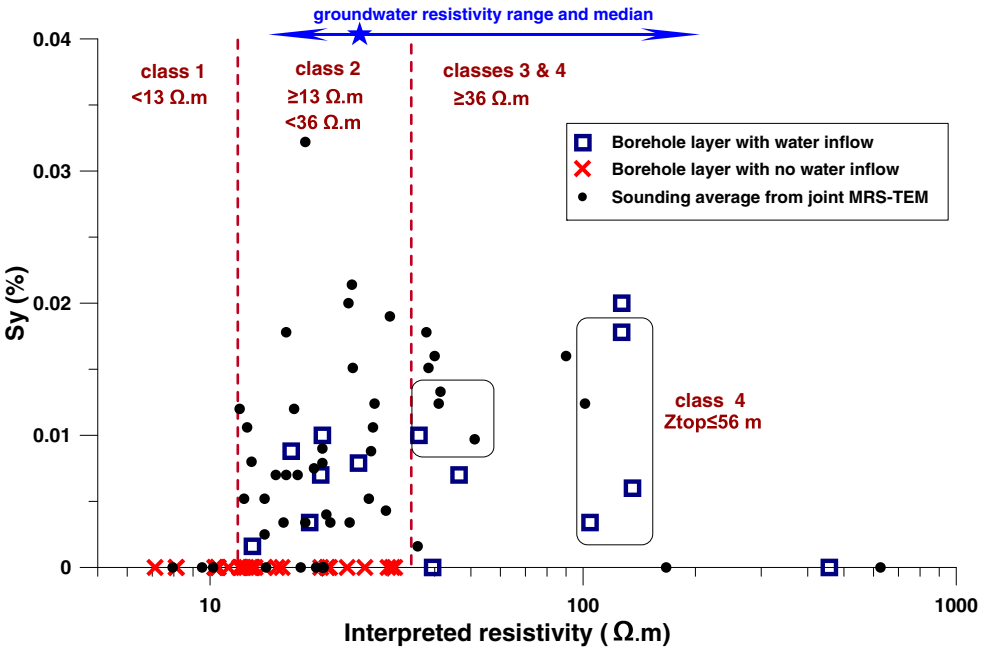

Fig. 6 S_y from MRS vs. resistivity from TEM soundings. Resistivity of circles is the average resistivity over the MRS aquifer thickness. Square and cross resistivities come from 17 joint MRS-TEM soundings with available lithologs. Z_{top} corresponds to the top of the aquifer layer or to the surface if there is no aquifer detected. Groundwater resistivity was measured in-situ with a conductivity probe

surface to the minimum between the depth of investigation from TEM and the depth of 80 m (maximum depth for local drilling rigs and MRS depth of investigation). The average MRS investigation depth is indeed about 78 m, which is calculated from the inversion software results and following the methodology of Legchenko et al. (2017). It was assumed, then, that the relationship between the resistivity and MRS results is valid to the depth of 80 m, even though some MRSs show an investigation depth of only 40–50 m.

The map displays the greatest potential for groundwater reserves (about 800 mm) to the northeast and southwest (Fig. 11a). The 2nd and 3rd resistivity-elevation classes are, however, associated with a high uncertainty regarding their S_y value (Table 1). Such a reserves map is therefore also uncertain, but not for areas with almost no reserves because the 1st resistivity-elevation class has never been linked with water inflow or strictly positive S_y.

The reserves shown on Fig. 11b were computed using only the 4th resistivity-elevation class, which is always associated with water inflow and strictly positive S_y. Patterns similar to the first reserves map can be observed, with high reserves, relative to the present dataset, in the northeastern and southwestern areas (300–700 mm). Such locations should be the best targets for borehole installation because they are relatively homogeneous and they are associated with only strictly positive S_y. The other small-size high-potential-reserve areas may be related to geological heterogeneities.

Discussion

Influence of hydrogeological fluctuations

The monitoring of hydrogeological components (rainfall, streamflow, aquifer) began in mid-2010. From this date to 2015, the four boreholes that were monitored as part of the study by Valois et al. (2017) displayed a stronger seasonal water level variation than an annual variation. Thus, one could assume that seasonal water level variation is stronger for the overall period considered (2009–2014). This seasonal variation is about 3 m at the maximum between the wet and the dry

Table 1 Water-inflow-presence rate from the layers of 55 lithologs, TEM data points and S_y properties from the 66 joint MRS-TEM soundings, and 17 lithologs-TEM-MRS data points for the four resistivity-elevation classes identified in Figs. 3 and 5

Class	Resistivity ρ (Ω m) and elevation Z_{top} (m asl) ranges	Water-inflow-presence rate	Non-zero S_y probability	Average S_y (%)
1	$\rho < 13$	0	0	0
2	$13 \le \rho < 36$	0.25	0.53	0.777
3	$36 \le \rho$; $Z_{top} > 56$ m	0.25	0.64	0.85
4	$36 \le \rho$; $Z_{top} \le 56$ m	1	1	1.06

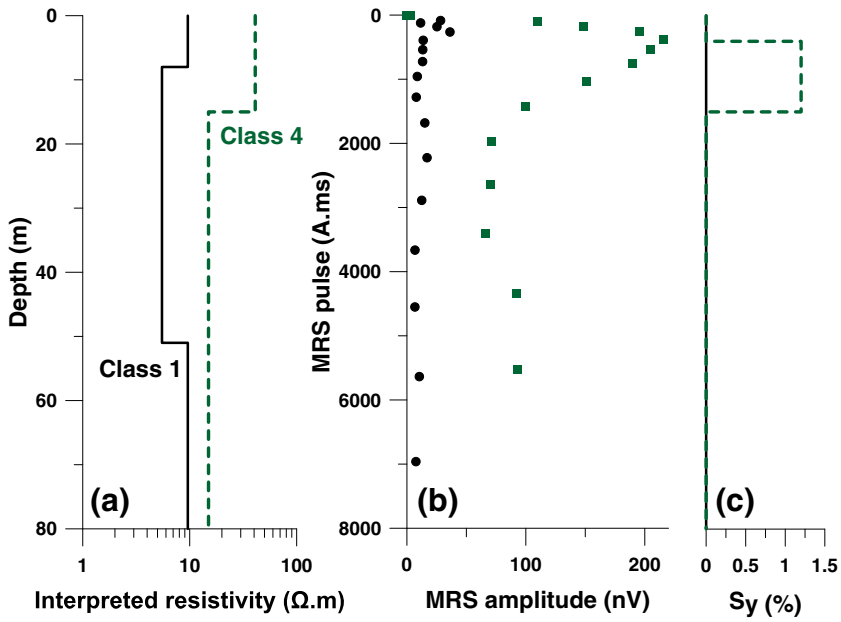

Fig. 7 Example of classes 1 and 4 data. Class 1 is represented with black lines and circles, whereas green-dashed lines and squares show class 4 data: **a** vertical resistivity models; **b** MRS amplitudes versus pulses (the greater the pulse, the deeper the penetration depth); **c** the S_y models derived from MRS data

season. The depth to water level at the four monitored sites was between 2 and 5 m below ground level.

Considering that the minimum depth of the water inflow layers is 10 m, then, the influence of the variation of the hydrogeological components on the litholog description was probably negligible. Regarding MRS and TEM measurements, a time-lapse survey on two sites was carried out with eight sampled periods during the year 2012 that comprised the groundwater low-level stage (end of the dry season: April) and the high-level stage (end of the monsoon: October). These results are not shown in this study, but both methods were not sensitive to such variations. It was concluded, therefore, that the hydrogeological variations were not enough to provoke changes in measurements, which could be due to the low sensitivity of the methods to shallow variations, and as well to low variations of the total water content in the zone of the water-table fluctuation. The amount of gravitational water through the S_y value is indeed low as compared to the MRS water content (Fig. 5).

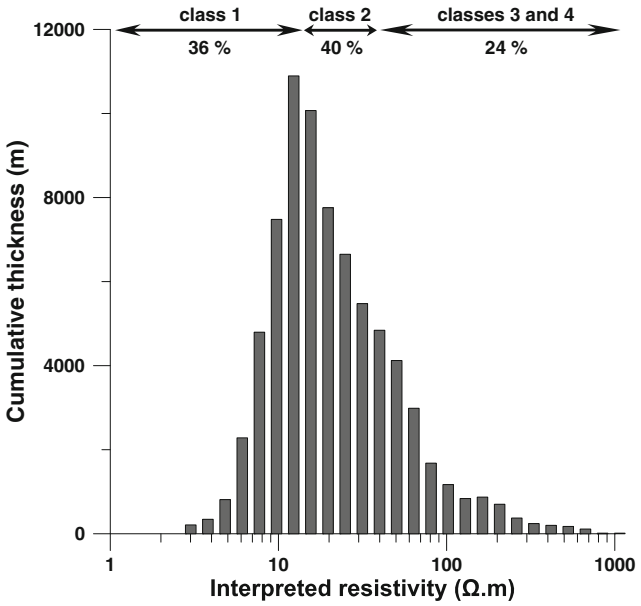

Fig. 8 Inverted resistivity histogram from the 612 TEM soundings. The cumulative thickness is the sum of layer thicknesses corresponding to a specific resistivity. Percentages correspond to the relative contribution of each class to the cumulative thickness histogram

Borehole siting success rates using TEM and MRS

Using MRS and TEM methods to site boreholes increases the success rate from 40 to 95%, as stated in the French Red Cross (2015) report. The unsuccessful 5% may be explained by local heterogeneities, which led to a significant drop in S_y for the drilled wells, although MRS indicates sufficient S_y at the sounding scale (100-m square loop). In addition, positive boreholes were drilled at two sites, although MRS signals were too weak to get a strictly positive S_y. Transmissive fractures with a water content too low to be identified with MRS could explain this phenomenon. These two sites are part of the 3rd class, which should then have a greater non-zero S_y probability.

By assuming that the presence or absence of S_y (Table 1) is directly linked to the borehole success rate, and that the 3rd and 4th classes are always associated with a strictly positive S_y, the borehole success rate is about 45% based on the proportion of each class in Fig. 8. This figure supports the 40% positive boreholes reported by French Red Cross (2015). Using only TEM would lead to a higher success rate because the highly conductive medium of class 1 would be avoided. In such a case, the success rate would be

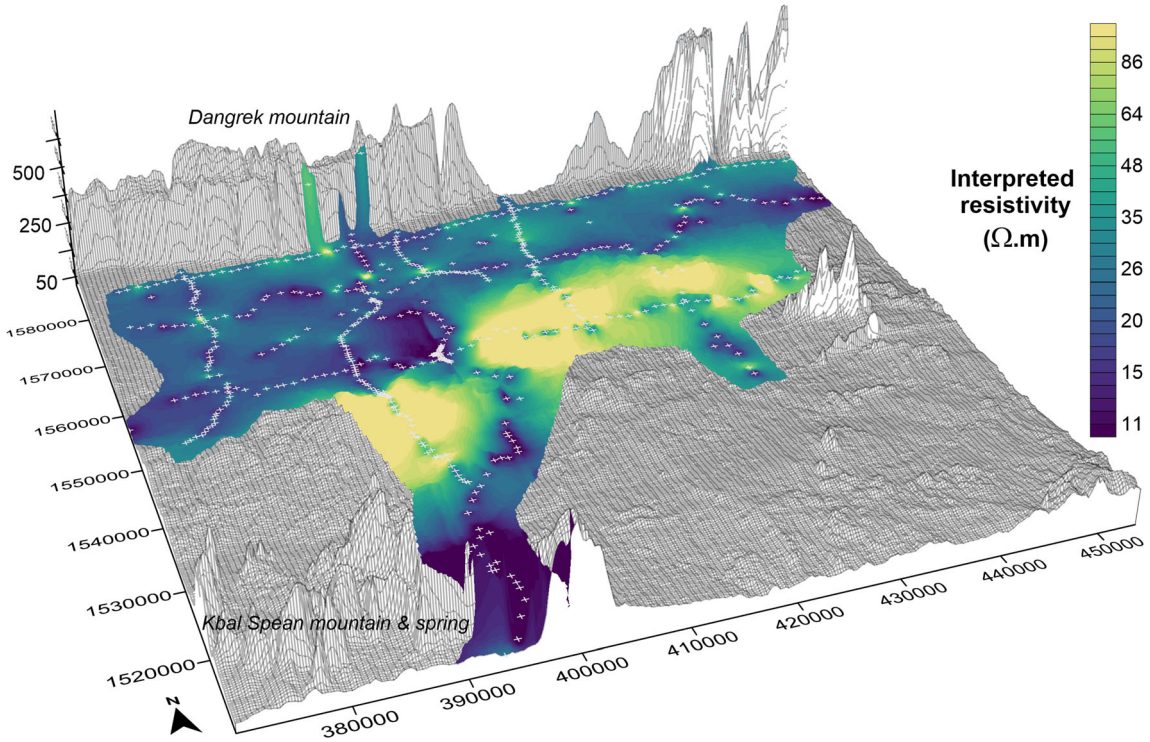

Fig. 9 Inverted resistivity of the first layer (0–3 m deep) superimposed on the topography map. Coordinates are in meters and the vertical scale is exaggerated 30 times. White crosses represent sounding locations. The coordinate reference system is WGS 84 UTM 48 N

approximately 70%. TEM without MRS could be used for targeting only class 4 resistive rocks, but this medium accounts for less than 24% of the TEM-encountered medium (Fig. 8). In fact, class 2 still represents 40% of the TEM-encountered medium, where resistivity cannot determine groundwater availability, as stated by the 47% null-S_y probability (Table 1). As a result, MRS is still necessary for class 2 to overcome such an obstacle.

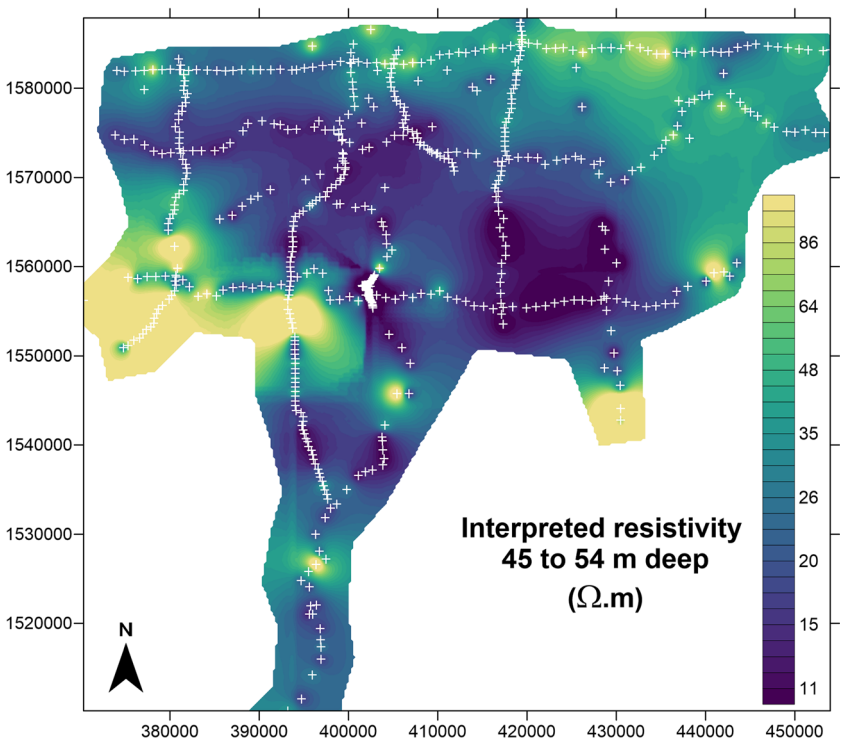

Fig. 10 Interpreted resistivity of the 10th layer (45–54 m deep). White crosses represent sounding locations. Coordinates are in meters. The coordinate reference system is WGS 84 UTM 48 N

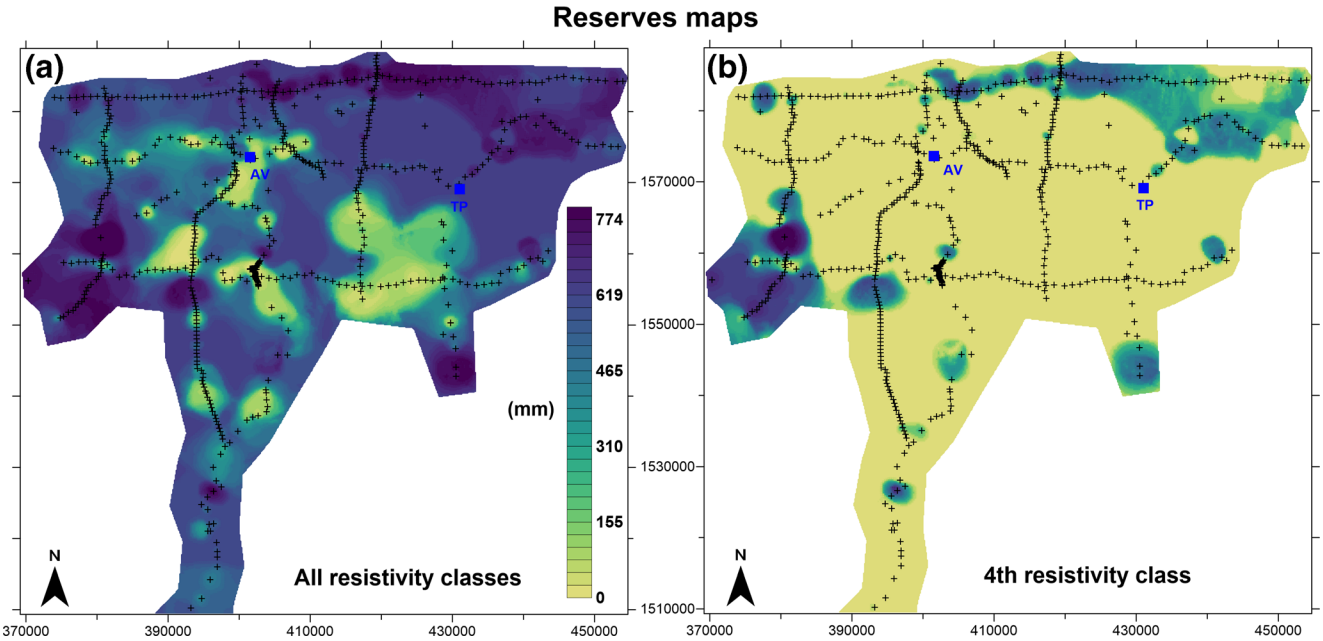

Fig. 11 Groundwater reserves maps computed from the 3D resistivity model. Black crosses represent sounding locations along roads mainly. Coordinates are in meters. AV and TP blue squares are Anlong Veng and Trapaing Prasat district capitals, respectively. **a** Computed with all resistivity-elevation classes from Table 1; **b** Computed with only the 4th resistivity-elevation class that is always associated with water inflow or strictly positive S_y. The coordinate reference system is WGS 84 UTM 48 N

Matrix versus fracture porosity

Primary and secondary porosity processes could be invoked to explain the hydrogeophysical behavior of materials described in this study. Class 1 materials and approximately half of the class 2 medium were never associated with gravitational water. The trends between sounding average resistivity and S_y (Fig. 6), as well as between water inflow layer resistivity and S_y, are positive for class 2 ($2.8\ 10^{-4}$ and $4.7\ 10^{-4}\ \Omega^{-1}$ m−1). This means that S_y (i.e., pore size) generally increases with resistivity, if S_y does not equal zero. Layers with no water inflow are, however, still present over the entire resistivity range of class 2. The role of resistivity in identifying three different hydrogeological behaviors should be explained by differences of rock type and clay content. The role of elevation in discriminating classes 3 and 4 results is also a finding of interest, although the water table is shallow and follows topography (mean of 4 m with a maximum of 8 m; Vouillamoz et al. 2015).

The matrix pore size could easily explain the behavior of class 1 material, which should correspond to rich clayey material with no gravitational water (null S_y and low resistivity). Class 2 behavior could be seen as a "transition zone", where enlargement of matrix pore size (higher S_y) may compete with its filling by fine-grained material (lower S_y). Reduced clay content (higher resistivity) and increased pore size (higher S_y) may explain the behavior of classes 3 and 4.

The competition of fractures filled with fine-grained material in clayey bodies (low S_y, low resistivity) with those open to water flows in low clayey media (high S_y, high resistivity) could as well explain the aforementioned results. The two positive boreholes that were drilled on negative MRS results (Fig. 6), as well as the fact that rock type (Figs. 2 and 3) cannot discriminate the water-inflow presence or absence, support the idea of a groundwater circulation dominated by fracture porosity. Transmissive fractures may indeed be invisible to MRS and may be mainly present below a fixed elevation. Cores drilled to a depth of 400 m by a mining company do in fact show that fracture density increases with depth; nevertheless, Samovar and AarhusInv inversion software used in this study assume vertical layered models to explain the results. With such assumptions, it is of course difficult to identify the fractures themselves. Zones with a high density of water-filled fractures could however generate data that are sufficiently different from data derived from the zones' surroundings (Legchenko et al. 2002). In this case, the model results (θ_{MRS}, resistivity) would correspond to some average over this layer. SCI would be well suited if there is a certain continuity (depth, thickness and/or fracture density) of this layer composed by a high density of water-filled fractures. Further investigation is needed to determine precisely the role of these two mechanisms regarding groundwater flow and storage.

Limitations of the study

A few trenches dug to a depth of 3 m by a mining company show small-scale geologic folds oriented east–west, with wavelengths of approximately 20 m. These spatial geological

variations seem important enough to raise questions about the spatial representativeness of the TEM soundings. Range values of experimental variograms vary from 3 to 6 km for the 20 resistivity layers inversed independently. Geological units may therefore have several variation wavelengths: one wavelength of a few tens of meters that could explain the small-scale folds and differences of nearby borehole yields and the 5% of negative boreholes despite positive MRS results (French Red Cross 2015), and another wavelength of several kilometers that impacts resistivities. Thus, uncertainty of the reserves maps (Fig. 11) could be high since the sources of uncertainties are multiple: small-scale structures that are invisible to geophysics such as fractures or folds, 3D interpolation of resistivities, relationships between S_y and resistivity, and uncertainties related to data acquisition and inversion. The largest source of uncertainty should be linked to the resistivity representativeness because of the low amount of TEM soundings in some areas, and the reliability of the inversions if groundwater flow is driven by a heterogeneous fracture-density field.

Because TEM is not very sensitive to shallow areas (5–10 m), near-surface sandy aquifers may not be well identified in the reserves map, although they may be productive areas to target for groundwater extraction. Such sands are present in the northeastern and southeastern portions of the study area; nevertheless, special care needs to be taken to protect these resources because they are very likely to be vulnerable to surface pollution. Moreover, groundwater must be managed sustainably because recharge is low and direct (Vouillamoz et al. 2015) with 28 mm/year on average, which corresponds to a small percentage of rainfall (1,796 mm/year on average, Valois et al. 2017).

Apart from TEM soundings, no information exists regarding deeper aquifers, even though some results indicate that groundwater resources may be higher in the fractured schist of the Paleozoic substratum, as compared to the surveyed Upper Triassic-Lower Cretaceous clayey sandstone (Vouillamoz et al. 2015). Resistive crystalline rock and sandstone units encountered at low elevations yield high S_y, which may be explained by a larger pore size in the matrix or fracture porosity in areas of low topography. Boreholes drilled at low topography, i.e., at the vicinity of the Stung Sreng stream and its tributaries, are in fact positive if such resistive media are encountered. Low topography areas may therefore be associated with efficient drainage for both surface runoff and groundwater flow.

Conclusions

This study adds to the hydrogeological knowledge of northwestern Cambodia through its comparison of lithologs, TEM, and MRS data sets. No clear link can be drawn between resistivity and geology because resistivity ranges of each geological unit overlap with at least one other unit. Nevertheless, sandstone and crystalline rocks seem to be the best targets for groundwater extraction because of high rates of water-inflow presence in the surveyed drilled holes. Low-elevation resistive mudstones, claystones, and schists are also linked to water inflow, especially at elevations below 56 m and resistivities greater than 36 Ω m where only water-inflow layers are encountered.

The MRS S_y approach, together with resistivity, made it possible to identify four resistivity and elevation classes with distinct S_y properties. The conductive class below 13 Ω m is in fact always associated with no S_y, whereas the resistive (≥36 Ω m) and low-elevation (≤56 m) class is always linked to strictly positive S_y, which may be explained by the clay content, which has low resistivity and non-drainable water, and by open fractures in resistive media, which is associated to higher S_y.

Using both MRS and TEM leads to almost a 100% chance of drilling a successful borehole, whereas without these geophysical methods, the success rate is only 45%. By avoiding the most conductive class, TEM would increase the success rate to approximately 70%, when it is carried out without MRS. The rate could reliably reach 100% by targeting only class 4 materials, but these media are encountered only in a few areas. Adding MRS measurements to TEM soundings is the best option for successfully siting borehole installations. Nevertheless, water-inflow layers evident in boreholes were not detected by MRS within two resistive bodies at high elevation; thus, one limit of the method described in this paper is a fractured medium with low water content that may be invisible to MRS.

The 612 TEM soundings highlight a mostly conductive medium of about 12 Ω m with some more resistive media that yields a log-average resistivity of 21 Ω m. Resistive areas are near the surface at the center of the map, whereas they are mainly at depth in the southwestern and northeastern areas of the map. These resistive areas coincide with the locations of upper Pleistocene sands and Paleozoic substrata.

The two groundwater reserves maps that were produced using the 3D resistivity model and the four resistivity-elevation classes show areas of greatest groundwater reserves, from 300 to 700 mm, with a very good probability of finding a non-zero S_y in the northeastern and southwestern portions of the second map. Areas with almost no reserves on the first map are also associated with a low uncertainty. Such information should be useful for government agencies and NGOs in the borehole siting process so as to better meet the needs of the communities; nevertheless, one should keep in mind that aquifers are poor in the overall area, as defined by low S_y, reserve and recharge values. Such aquifers, if present, can in general deliver enough water for domestic needs. Those needs are estimated to be 1.5 mm/year by assuming a daily consumption of 100 L per capita and a population that has doubled since

2008 in the studied area. If this domestic need is low compared to the average annual recharge (28 mm) and reserve (173 mm), using groundwater for irrigation of rice crops should be limited to specific locations with productive aquifers (Vouillamoz et al. 2015).

Finally, this study improved the knowledge of the links between geology, electrical resistivity and hydrogeological parameters. It allowed the researchers to develop a new methodology, with the creation of the first groundwater reserves maps for the Oddar Meanchey province. Improving geological maps through the use of more lithologs and geophysical data sets may provide a good solution for better assessing and reducing the uncertainties of these reserve maps.

Acknowledgements We thank Vincent Dhiver who managed the second project and S. Sokheng and P. Sophoeun for their efficient assistance in field work. Also we thank the Institut de Technologie du Cambodge (ITC) for their assistance in field work during several internships. Lastly, we thank A. Petibon and L. Anstett for making this project feasible.

Funding Information This work has been carried out in the framework of the Institut de Recherche pour le Développement and the French Red Cross collaborative project 39842A1 - 1R012-RHYD, with the financial support of the European Community (grant DIPECHO SEA ECHO/DIP/BUD/2010/01017 and grant DCI-FOOD/2011/278-175).

References

Auken EA, Christiansen V, Jacobsen L, Sørensen KI (2005) Laterally constrained 1D inversion of 3D TEM data: Symposium on the Application of Geophysics to Engineering and Environmental Problems (SAGEEP) proceedings, April 2005, Atlanta, GA, pp 519–524

Auken EA, Christiansen AV, Fiandaca G, Schamper C, Behroozmand AA, Binley A, Nielsen E, Effersø F, Christensen NB, Sørensen KI, Foged N, Vignoli G (2015) An overview of a highly versatile forward and stable inverse algorithm for airborne, ground-based and borehole electromagnetic and electric data. Explor Geophys 2015:223–235

Baroncini-Turricchia G, Francés AP, Lubczynski MW, Martínez Fernández J, Roy J (2014) Integrating MRS data with hydrologic model: Carrizal catchment (Spain). Near Surf Geophys 12:255–269. https://doi.org/10.3997/1873-0604.2014003

Barsukov P, Fainberg E, Khabensky E (2006) Shallow investigations by TEM-FAST technique: methodology and examples. In: Spichak V (ed) Electromagnetic sounding of the Earth's interior, methods in geochemistry and geophysics, 40. Elsevier, Amsterdam, pp 55–77

Bedrosian PA, Schamper C, Auken E (2016) A comparison of helicopter-borne electromagnetic systems for hydrogeologic studies. Geophys Prospect 64(1):192–215

Benner SG, Polizzotto ML, Kocar BD, Ganguly S, Phan K, Ouch K, Sampson M, Fendorf S (2008) Groundwater flow in an arsenic-contaminated aquifer, Mekong Delta, Cambodia. Appl Geochem 23:3072–3087

Berg M, Stengel C, Trang PTK, Hung Viet P, Sampson ML, Leng M, Samreth S, Fredericks D (2007) Magnitude of arsenic pollution in the Mekong and Red River deltas: Cambodia and Vietnam. Sci Total Environ 372:413–425. https://doi.org/10.1016/j.scitotenv.2006.09.010

Bernard J (2007) Instruments and field work to measure a magnetic resonance sounding. Bol Geol Min 118(3):459–472

Bouche VA, Lartsev VS, Boulatov VE, Volodina VI, Catinsky YG, Veselov V (1990) Carta Cosmogeologique du Cambodge [Cosmogeological map of Cambodia]. JSC VNIIZARUBEZHGEOLOGIA, Moscow

Bunthan N (2006) A review of the current situation for water resources management and the role of agricultural education in Cambodia. J Dev Sustain Agric 1:25–33

Chongo M, Christiansen AV, Fiandaca G, Nyambe IA, Larsen F, Bauer-Gottwein P (2015a) Mapping localised freshwater anomalies in the brackish paleo-lake sediments of the Machile–Zambezi Basin with transient electromagnetic sounding, geoelectrical imaging and induced polarisation. J Appl Geophys 123:81–92

Chongo M, Christiansen AV, Tembo A, Banda KE, Nyambe IA, Larsen F, Bauer-Gottwein P (2015b) Airborne and ground-based transient electromagnetic mapping of groundwater salinity in the Machile–Zambezi Basin, southwestern Zambia. Near Surf Geophys 13(4):383–395

Dottin O (1972) Carte géologique de reconnaissance: Siem Reap [Geological map: Siem Reap]. BRGM, Orléans, France

French Red Cross (2015) Final narrative report no. 3-2014-2015. DCI-FOOD/2011/278–175, French Red Cross, Paris, 184 pp

Guéguen Y, Palciauskas V (1997) Introduction à la physique des roches [Introduction to rock physics]. Hermann, Paris, 312 pp

Gupta AD (2001) Challenges and opportunities for water resources management in Southeast Asia. Hydrol Sci J 46(6):923–935

Hunter D, Kepic A (2005) Surface nuclear magnetic resonance signal contribution in conductive terrains. Explor Geophys 36(1):73–77

Johnston R, Roberts M, Try T, de Silva S (2013) Groundwater for irrigation in Cambodia. http://www.iwmi.cgiar.org/Publications/issue_briefs/cambodia/issue_brief_03-groundwater_for_irrigation_in_cambodia.pdf. Accessed 20 March 2015

Kirsch R (ed) (2006) Groundwater geophysics, a tool for hydrogeology. Springer, Heidelberg, Germany

Kummu M, Tes S, Yin S, Adamson P, Josja J, Koponen J, Richey J, Sarkkula J (2014) Water balance analysis for the Tonle Sap Lake-floodplain system. Hydrol Process 28:1722–1733

Landon M (2011) Preliminary compilation and review of current information on groundwater monitoring and resources in the lower Mekong River basin. USGS, Reston, VA

Legchenko A, Valla P (2002) A review of the basic principles for proton magnetic resonance sounding measurements. J Appl Geophys 50(1):3–19

Legchenko A (2013) Magnetic resonance imaging for groundwater. Wiley, Chichester, UK, 235 pp

Legchenko A, Baltassat JM, Beauce A, Bernard J (2002) Nuclear magnetic resonance as a geophysical tool for hydrogeologists. J Appl Geophys 50(1):21–46

Legchenko A, Ezerski A, Girard JF, Baltassat JM, Boucher M, Camerlynk C, Al-Zoubi A (2008) Interpretation of magnetic resonance soundings in rocks with high electrical conductivity. J Appl Geophys 66:118–127. https://doi.org/10.1016/j.jappgeo.2008.04.002

Legchenko A, Ezersky M, Camerlynck C, Al-Zoubi A, Chalikakis K (2009) Joint use of TEM and MRS methods in a complex geological setting. Compt Rendus Geosci 341(10):908–917

Legchenko A, Vouillamoz JM, Lawson FMA, Alle C, Descloitres M, Boucher M (2016) Interpretation of magnetic resonance measurements in the varying earth's magnetic field. Geophysics 81(4):23–31

Legchenko A, Comte JC, Ofterdinger U, Vouillamoz JM, Lawson FMA, Walsh J (2017) Joint use of singular value decomposition and Monte-Carlo simulation for estimating uncertainty in surface NMR inversion. J Appl Geophys 144:28–36

Lenat J, Fitterman D, Jackson D, Labazuy P (2000) Geoelectrical structure of the central zone of piton de la Fournaise volcano (Reunion). B Volcanol 62:75–89

Lienert B (1991) An electromagnetic study of Maui's last active volcano. Geophysics 56:972–982

Lubczynski M, Roy J (2007) Use of MRS for hydrogeological parameterization and modelling. Bol Geol Min 118(3):509–530

MacNeil R, Sanford W, Connor C, Sandberg S, Diez M (2007) Investigation of the groundwater system at Masaya Caldera, Nicaragua, using transient electromagnetics and numerical simulation. J Volcanol Geotherm Res 166:217–232

McNeill J (1980) Electrical conductivity of soils and rocks, technical note TN-5. Geonics, Mississauga, ON, 22 pp

MRD, JICA (2002) The study on groundwater development in southern Cambodia: final report. JICA, Tokyo

Nabighian MN (1988) Electromagnetic methods in applied geophysics, vol 1. Society of Exploration Geophysicists, Tulsa, OK

Nabighian MN (1991) Electromagnetic methods in applied geophysics, vol 2. Society of Exploration Geophysicists, Tulsa, OK

National Institute of Statistics (2009) Cambodia: general population census of Cambodia 2008 no. DDI-KHM-NIS-GPCC-2008-v1.0. Ministry of Planning, Phnom Penh, Vietnam. https://camnut.weebly.com/uploads/2/0/3/8/20389289/2009_census_2008.pdf. Accessed 19 March 2015

Pryet A, Dominguez C, Tomai PF, Chaumont C, d'Ozouville N, Villacís M, Violette S (2012) Quantification of cloud water interception along the windward slope of Santa Cruz Island, Galapagos (Ecuador). Agric For Meteorol 161:94–106

Pryet A, d'Ozouville N, Violette S, Deffontaines B, Auken E (2012) Hydrogeological settings of a volcanic island (San Cristóbal, Galapagos) from joint interpretation of airborne electromagnetics and geomorphological observations. Hydrol Earth Syst Sci 16(12): 4571–4579

Raksmey M, Jinno K, Tsutsumi A (2010) Influence of flooding on groundwater flow in central Cambodia. Environ Earth Sci 63: 151–161

Rasmussen WC, Bradford GM (1977) Ground-water resources of Cambodia. US Geol Surv Water Suppl Pap 1608-P. http://pubs.er.usgs.gov/publication/wsp1608P. Accessed 20 March 2015

Schirov M, Legchenko A, Creer G (1991) New direct non-invasive ground water detection technology for Australia. Explor Geophys 22:333–338. https://doi.org/10.1071/EG991333

Shushakov OA (1996) Surface NMR measurement of proton relaxation times in medium to coarse-grained sand aquifer. Magn Reson Imaging 14(7–8):959–960

Trushkin DV, Shushakov OA, Legchenko AV (1995) Surface NMR application to an electroconductive medium. Geophys Prospect 43: 623–633

Valois R, Vouillamoz JM, Lun S, Arnout L (2017) Assessment of water resources to support the development of irrigation in northwest Cambodia: a water budget approach. Hydrol Sci J 62 (11):1840–1855

Viezzoli A, Christiansen AV, Auken E, Sørensen K (2008) Quasi-3D modeling of airborne TEM data by spatially constrained inversion. Geophysics 73(3):F105–F113

Vouillamoz JM, Descloitres M, Bernard J, Fourcassier P, Romagny L (2002) Application of integrated magnetic resonance sounding and resistivity methods for borehole implementation: a case study in Cambodia. J Appl Geophys 50(1):67–81

Vouillamoz JM, Favreau G, Massuel S, Boucher M, Nazoumou Y, Legchenko A (2008) Contribution of magnetic resonance sounding to aquifer characterization and recharge estimate in semiarid Niger. J Appl Geophys 64(3):99–108

Vouillamoz JM, Sokheng S, Bruyere O, Caron D, Arnout L (2012) Towards a better estimate of storage properties of aquifer with magnetic resonance sounding. J Hydrol 458–459:51–58

Vouillamoz JM, Sophoeun P, Bruyere O, Arnout L (2013) Estimating storage properties of aquifer with magnetic resonance sounding: a field verification in northern Cambodia of the gravitational water apparent cutoff time concept. Near Surf Geophys 12:211–216

Vouillamoz JM, Valois R, Lun S, Caron D, Arnout L (2015) Can groundwater secure drinking water supply and supplementary irrigation in new settlements of North-West Cambodia? Hydrogeol J. https://doi.org/10.1007/s10040-015-1322-6